JOURNAL OF AGRICULTURAL AND FOOD CHEMISTRY

J. Agric. Food Chem. **2004,** *52,* 4979−4983 **4979**

Magnetic Resonance Imaging of Seeds by Use of Single Point Acquisition

MARCO L. H. GRUWEL,*,† PETER LATTA,†,‡ VYACHESLAV VOLOTOVSKYY,† MILOŠ ŠRAMEK,§ AND BOGUSLAW TOMANEK†,||

NRC Institute for Biodiagnostics, 435 Ellice Avenue, Winnipeg, MB R3B 1Y6, Canada, Slovak Academy of Sciences, Institute for Measurement Science, Dúbravská cesta 9, SK-84219 Bratislava, Slovakia, OAW Visualisierung, Donau-City Strasse 1, A-1220 Vienna, Austria, and NRC Institute for Biodiagnostics (West), Room B153, 3330 Hospital Drive N.W., Calgary, AB T2N 4N1, Canada

In general, magnetic resonance imaging (MRI) is used to obtain a spatial representation of the water distribution in an object. Water in soft materials (living matter) often shows a high degree of translational mobility, giving rise to relatively long magnetic relaxation times. This allows the use of conventional MRI techniques such as the spin−echo, to acquire an image. However, when hydration levels become low, water becomes less mobile, resulting in much shorter magnetic relaxation times and a corresponding signal loss. To avoid problems arising from rapid decaying signals, we investigated the use of single point imaging (SPI) in the study of seeds. We were able to obtain SPI images of nonimbibed and imbibed seeds. Using SPI with shaped gradients significantly reduced the acoustic noise level.

KEYWORDS: Hydration; MRI; SPI; spin-echo; acoustic noise; shaped gradients

1. INTRODUCTION

Seed moisture content and storage temperature are considered the main factors in maintaining seed viability. When in contact with water, either directly through wetting or through contact with moist air, seeds will start to accumulate water. Many factors can influence this process, among them are the seed coat composition and permeability, temperature, and hydrostatic pressure (*1*). It has been known for some time now that an increase in moisture level could result in a compromised seed viability (*2*). Due to its potentially large economical impact, especially for staple grains such as wheat and barley, loss of viability is of concern to both producers and end users. Knowledge of seed moisture, and most importantly knowledge of the moisture distribution within the seed, is thus essential.

Localization and measurement of water content in seeds is often obtained using invasive and destructive techniques. The most common techniques to monitor water uptake are based on the use of ^3H_2O, iodine staining, or the use of Mn^{2+} as a tracer added to the imbibition water (*3*). MRI offers the possibility to study the water distribution in seeds noninvasively (*4*) and has also proven to be an excellent tool to study the water distribution in food stuffs (*5*, *6*) and seeds (*4*) with a relatively high moisture content. Using conventional frequency encoding (spin−echo) MRI techniques, detailed moisture maps, as well as information on water dynamics (relaxation parameters, diffusion constants), could be obtained. However, at reduced moisture levels, water dynamics reduces significantly, resulting in line broadening. Spin−spin relaxation times (T_2, T_2^*) can become so short that the resonance amplitude decreases below the limit of detection with standard techniques. In general, at such low levels of hydration, the efficiency of spin−echo MRI techniques becomes very limited (*7*).

Obtaining noninvasive information on seed hydration in the early stages of imbibition, or in general at relative low moisture levels, is thus a challenge. Detailed knowledge of water movement during this development phase is not available. This knowledge, however, could, for instance, significantly aid the development of osmotic priming techniques. Osmotic priming improves seed germination under adverse conditions as well as good conditions and basically prepares the seed for an accelerated germination when planted (*8*, *9*). Another example would be in the area of viability testing of barley samples. It was recently shown that the loss of barley viability during storage could be detected within 3−4 h of imbibition, using NMR relaxation time measurements of the whole kernel (spectroscopy) (*4*). These measurements correlated with a rapid water uptake in the area between the seed embryo and endosperm, as shown by MRI. However, using conventional spin−echo experiments, we were not able to detect this until much later in the germination process.

To observe signals from condensed matter, Emid and Creyghton (*10*) developed a single point imaging (SPI) tech-

* To whom correspondence should be addressed. E-mail: marco.gruwel@nrc-cnrc.gc.ca.
† NRC Institute for Biodiagnostics.
‡ Slovak Academy of Sciences.
§ OAW Visualisierung.
|| NRC Institute for Biodiagnostics (West).

10.1021/jf049078f CCC: $27.50
Published on Web 07/16/2004

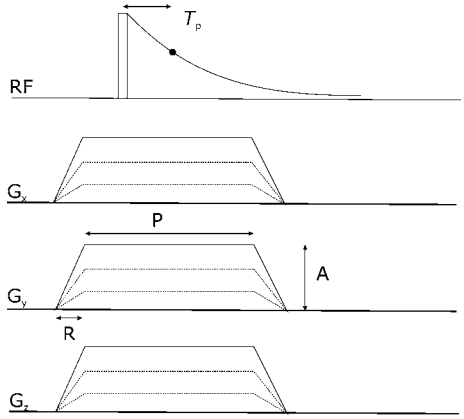

Figure 1. Typical single point imaging sequence. T_p is the time of acquisition after the RF α excitation. Three orthogonal gradients are shown for 3D SPI. *R* indicates the ramp time, *A*, the gradient amplitude, and *P*, the time during which the gradient is stable.

nique. This is a pure phase-encoding technique in which a single point of the magnetic resonance signal is acquired after a short encoding time in the presence of a gradient. The encoding time can be made very short in comparison with the time delays employed in conventional spin−echo experiments. SPI, or constant time images, are free from distortions caused by line broadening effects such as $\boldsymbol{B_0}$ inhomogeneities, chemical shifts, and other time-dependent interactions. Resolution and sensitivity are in principle determined by the gradient strength and the dead time of the coil (*11*). During the past few years, interest in SPI applications has picked up (*12*), and several significant improvements have been implemented (*13*, *14*).

Neither SPI nor its recent improvement have been used to obtain images of seeds with low moisture content. The aim of this work is to show that SPI can be used to obtain information on the water distribution in seed samples where conventional spin−echo experiments fail. With SPI, the water distribution in seeds can be obtained from the start of the imbibition up to the time point at which full hydration occurs. This has not been possible with conventional spin−echo techniques and hampered early investigations into water uptake in seeds (*4*). In addition, we introduce the use of shaped gradients to significantly reduce acoustic noise levels during the SPI measurements.

2. MATERIALS AND METHODS

2.1. Instrumentation. All MRI experiments were performed on an 11.7 T (500 MHz) Magnex (Magnex Scientific Ltd., Yarnton, UK)

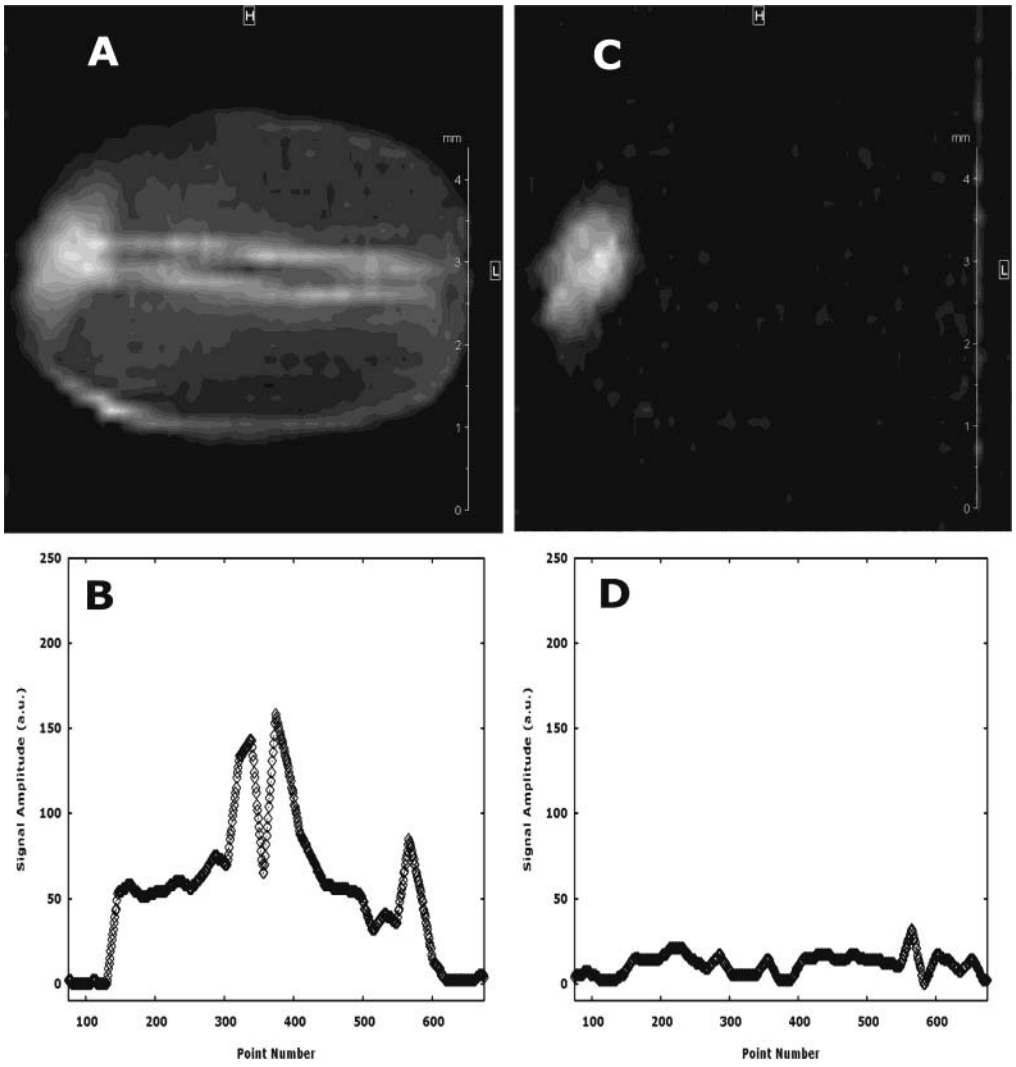

Figure 2. (**A**) One slice from a 3D spin–echo experiment (see Materials and Methods for details) of a wheat kernel after imbibition in water. The embryo can easily be recognized on the left. The seed crease can easily be identified by the parallel bands through the images. (**B**) Signal intensity of the water resonance going from top to bottom through the center of **A**. (**C**) Slice, at the same orientation as **A**, obtained after overnight drying. The same MRI sequence and parameters were used as in **A**. (**D**) Same profile as **B**, but for a dry kernel.

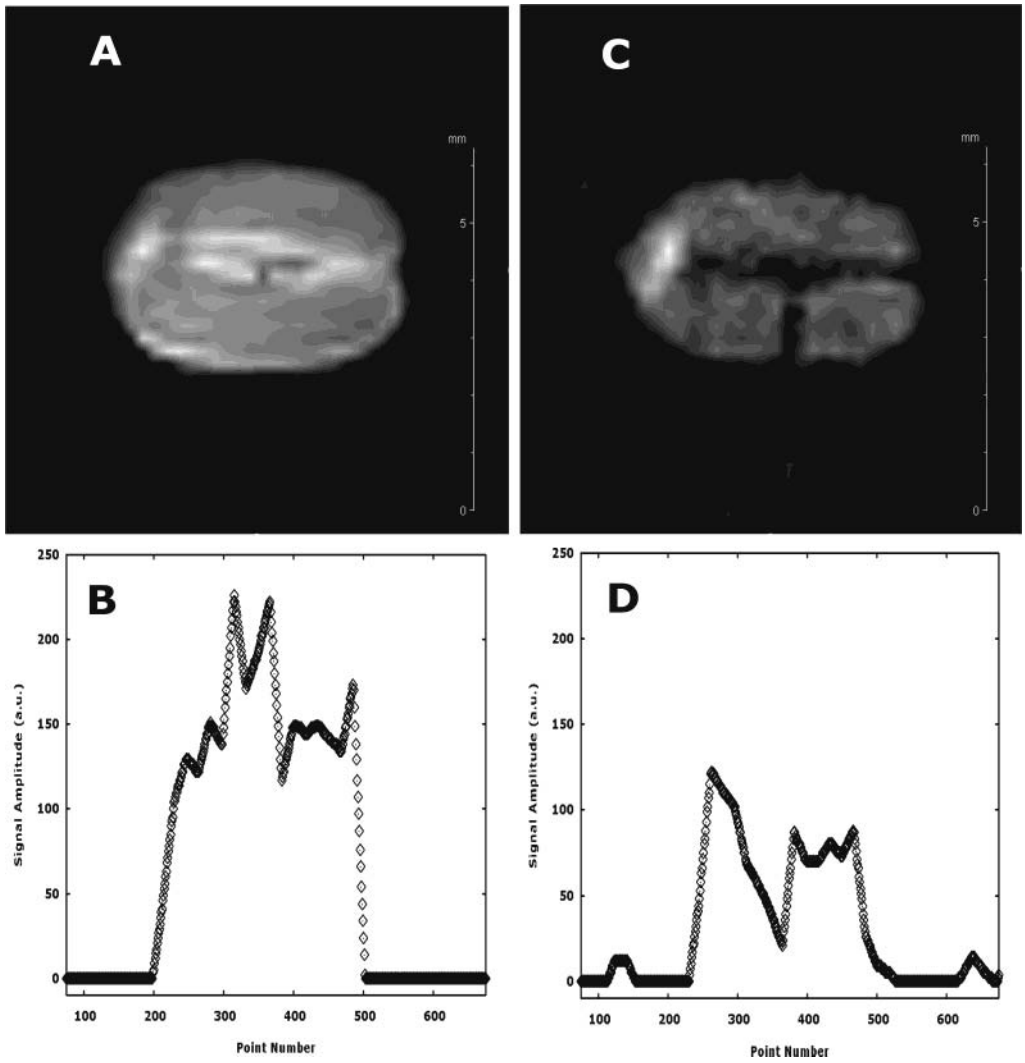

Figure 3. (**A**) One slice from a 3D SPI image (see Materials and Methods for details) of the same wheat kernel as that used in **Figure 2**, after imbibition in water. The embryo can easily be recognized on the left. As in **Figure 2**, the seed crease can also be recognized. (**B**) Signal intensity of the water resonance going from top to bottom through the center of **A**. (**C**) SPI image obtained after overnight drying. The same MRI sequence and parameters were used as in **A**. (**D**) Same profile as **B**, but for the dry kernel.

vertical bore magnet equipped with a Magnex SGRAD 123/72/S 72 mm self-shielded, water cooled, gradient set producing a maximum gradient strength of 550 mT · m^{-1}. A Bruker (Milton, ON) Avance DRX console with a ParaVision2.1.1 operating system was interfaced to the magnet. The probe and coil (Helmholtz configuration; 7-mm i.d.) were home-built. All experiments were performed at room temperature (20 °C).

2.2. Sample Handling. Prior to imaging, A. C. Barrie (*Triticum aestivum*) wheat kernels were imbibed in water for 18 h. For microimaging, an imbibed seed was carefully dried at the surface, by application of only slight pressure and use of a paper towel. After drying, the seed was glued onto the inner surface of a small glass cylinder (7-mm o.d.) which could be inserted into the probe. Immediately after insertion into the probe, the imbibed seed was imaged. After imaging with the 3D spin−echo and the SPI sequences was performed, the kernel was left overnight to dry in the magnet, using (low flow) dry N_2 gas. The next day, the dried wheat kernel was imaged again, using the exact same pulse sequences and parameters. Seed moisture levels were determined with the standard ASAE procedure for unground grain and seeds (ASAE S352.2) (*15*). The imbibed kernels contained 66.4% db moisture while the samples left to dry overnight in the magnet contained only 12.48% db moisture.

2.3. Microimaging. Images were obtained using a conventional 3D spin−echo and the SPI (3D) sequence. The 3D spin−echo sequence used a hard (100 μs) excitation and a slice selective Gaussian (200 μs) refocusing pulse with a 2.7 ms echo time, a 128 × 64 × 16 points data matrix, and an FOV of 1.2 × 0.8 × 0.8 cm^3. The average of two signals was acquired in 7 min.

In contrast to standard 2D spin−echo imaging, SPI does not employ slice selective pulses, which require a long duration. SPI relies on the acquisition of a single time domain point after signal excitation with a short radio frequency pulse (see **Figure 1**) of duration T_p and flip angle α. Since the RF pulse is applied while the gradient is on, its duration must be short enough to excite all frequencies selected by the gradient (*11*). All spatial encoding in SPI is done through phase encoding, resulting in gradient switching for each data point in the final image. Using linear gradient ramps of short duration R (see Figure 1), excessive acoustic noise and gradient vibration can be an annoying side effect of SPI. To avoid these problems, Balcom et al. (*13*) developed the SPRITE modification of SPI. SPRITE employs a discrete stepping of the gradients from $\pm A_m$ to $\mp A_m$, with A_m representing the maximum gradient amplitude, without turning the gradient current off. A drawback of this technique is the rapid heating of the gradient set due to the continuous gradient current. To avoid problems with acoustic noise, gradient set vibrations, and gradient set overheating, we developed an SPI modification that uses shaped, sinusoidally modulated gradient ramps (*16*).

SPI experiments were performed with a data matrix of 64 × 64 × 32 points for an FOV of 1.4 × 1.4 × 1.4 cm^3. Note that these parameters are slightly different from the spin−echo experiments, to avoid excessive heating of the gradient set due to the strong gradients. The detection time, T_p (see **Figure 1**), was 200 μs, and T_R was set to 10

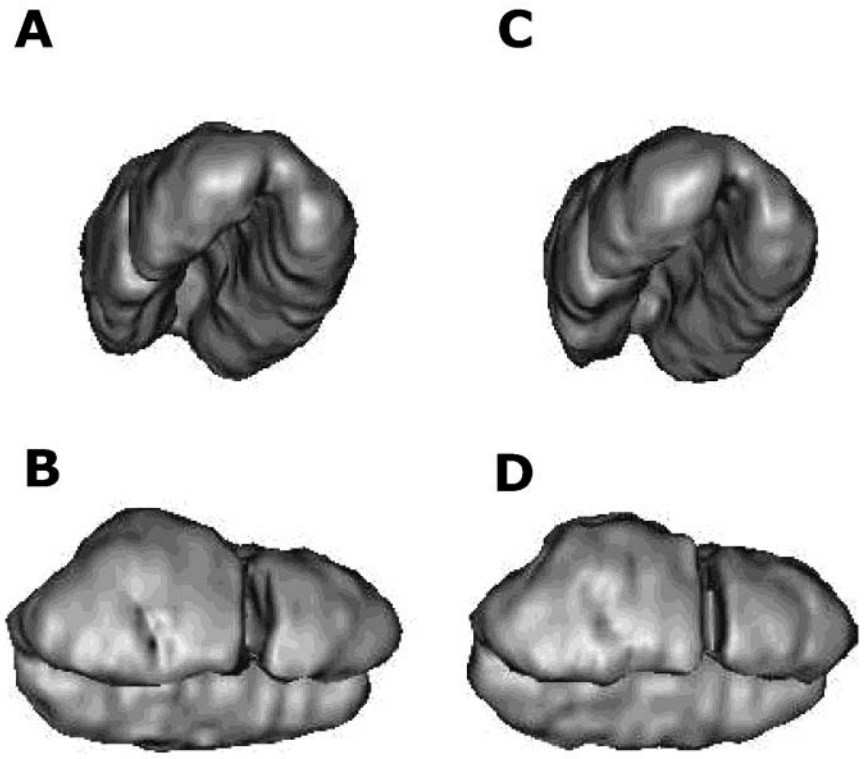

Figure 4. Two 3D SPI reconstructions, (**A**, **B**) using sinusoidal ramped gradients and (**C**, **D**) using linear ramped gradients. Note that the reconstructions for both orientations are indistinguishable; however, the acoustic noise level of the acquisition in **A** and **B** was significantly lower than that for **C** and **D**.

ms. A gradient ramp time, *R*, of 1.4 ms was selected for all SPI experiments. The slope of the ramp was either linear or sinusoidal. The total duration of these 3D SPI experiments was 22 min.

3. RESULTS AND DISCUSSION

In condensed matter, most often the spin−lattice relaxation time T_1, is long compared to the spin−spin-relaxation time ($T_1 \gg T_2$, T_2^*). In our experiments, T_R, the repetition time, was selected such as to ensure that all transverse magnetization had disappeared prior to the next excitation. Using the notation of **Figure 1**, the signal intensity *S* from the local spin density ρ at a point in the SPI image is given by (*17*)

$$S_{SPI}(T_p) = \rho \exp\left(-\frac{T_p}{T_2^*}\right) \cdot \left(\frac{1 - \exp\left(-\frac{T_R}{T_1}\right)}{1 - \cos\alpha \exp\left(-\frac{T_R}{T_1}\right)} \cdot \sin\alpha\right) \quad (1)$$

$S_{SPI}(T_p)$ has an optimum for $\cos\alpha = \exp(-T_R/T_1)$, the Ernst-angle. Careful selection of the time delays T_p and T_R introduces spin−spin and spin−lattice relaxation weighting into the images, respectively. In the case of a spin−echo experiment, the signal intensity can be described by

$$S_{SE}(T_E) = \rho \exp\left(-\frac{T_E}{T_2}\right) \cdot \left(1 - \exp\left(-\frac{T_R}{T_1}\right)\right) \quad (2)$$

with TE defining the echo time and assuming that diffusion can be ignored. Thus, in the case where $T_1 > T_R > T_2$, SPI has a major advantage over the conventional spin−echo. Gravina and Cory (11) provide a more detailed discussion on the advantages of SPI over the conventional spin−echo.

Parts **A** and **C** of **Figure 2** show a slice of the same wheat kernel when wet and dry, respectively, obtained with the 3D spin−echo experiment. The orientation of the slices is exactly the same. One can clearly observe the difference in water distribution between the two images. The slice thickness was 0.5 mm, and the in-plane resolution was $94 \times 125\ \mu m^2$. After 24 h of drying in the probe, most water left in the wheat kernel seems to reside in the embryo (see **Figure 2C**). The endosperm hardly shows any signal amplitude from water. Of course, this is in part due to the lowered water content in the endosperm after drying. However, the small amount of water that is still present in the endosperm is now strongly interacting with the solid phase, significantly reducing the water magnetic relaxation times. Water T_2 in that case could be so short that most signal has decayed before echo formation would be possible (*18*, *19*). Equation 2 shows that signal intensity of the spin−echo sequence rapidly decays when $T_E \approx T_2$. In SPI, on the other hand, T_p can be made as short as possible and is only limited by hardware restrictions.

To avoid problems with short relaxation times, we also measured the same wheat kernel using SPI. Parts **A** and **C** of **Figure 3** show SPI slices of the wet and the dry wheat kernel, respectively. Both images were acquired with linearly ramped gradients. The in-plane resolution of the images is $219 \times 219\ \mu m^2$ for a slice thickness of 0.48 mm. Again, as in the case for the spin−echo sequence, the difference in signal intensity for wet and dry kernel is clearly visible. However, in contrast with the spin−echo experiments, SPI of the dry wheat still shows signal amplitude in the endosperm. Equation 1 explains that as long as $T_p \leq T_2^*$, the excited magnetization will not all have vanished, and images can still be obtained. For the dry, whole wheat kernel, we measured a T_2^* of $\sim$250 μs, which is indeed still larger than T_p. **Figure 3** also clearly shows the difference in size between a hydrated and dry kernel. During the drying process, part of the endosperm of the kernel separated, as can be seen in **Figure 3C**. Note that such effects cannot be detected using standard spin−echo experiments. Often these deficits

cannot be detected by visual inspection, as they remain hidden under the seed coat or hull. For comparison, **Figure 2**, parts **B** and **D,** and **Figure 3**, parts **B** and **D,** also show the relative water signal intensity obtained from the images for a cross section of the kernel perpendicular to its long-axis, through the center of the wheat kernel. **Figures 2B** and **3B** clearly show the water abundance in the seed crease area and the skin. The latter more pronounced in the lower parts of the images of **Figures 2A** and **3A**. These areas are well-known to accumulate water (*2*).

Two different views of the 3D reconstruction of the SPI data are shown in **Figure 4**. Details of the 3D reconstruction have been described by Šramek et al. (*20*). Parts **A** and **B** of **Figure 4** are reconstructions from data acquired with sinusoidal ramped (silent) gradients, while parts **C** and **D** of **Figure 4** were acquired with linear ramped gradients. The quality of the reconstructions is indistinguishable; however, the acoustic noise level for the shaped gradient experiment was significantly lower than that for the linear ramped experiment. Details of this experiment are beyond the scope of this publication and will be published elsewhere (*16*). As shown in the 2D image of **Figure 3C**, the small crack in the endosperm can clearly be observed in the 3D reconstruction shown in **Figure 4**, parts **B** and **D**. SPI could thus be used as a valuable tool to study seed-imperfections.

The only drawback of using SPI, compared to the spin−echo, is the inefficient way of sampling the data. However, new k-space sampling techniques are being developed and will shorten the time to acquire the images significantly. Imaging sequences incorporating rapid gradient switching often generate acoustic noise with a relative high sound pressure level. As addressed previously, this can be reduced by special gradient ramping (*13*). However, this could cause heating of the gradient set. We introduced the use of shaped gradients to reduce acoustic noise. This modification does provide a significant reduction in acoustic noise and does not lead to excessive gradient set heating (*16*). In **Figure 3**, we show that SPI gradient ramping, be it linear or shaped, results in indistinguishable images.

In conclusion, we have shown that SPI can be used to nondestructively study water uptake in seeds from the start of imbibition. MRI images of seeds with only 12.5% (d.b.) moisture content were presented, showing the actual contours of the seed and not just that of the embryo. Using a sinusoidal gradient shape caused significant reduction of acoustic noise, ensuring that SPI can be used in any laboratory without the risk of damage to the MRI equipment.

ABBREVIATIONS USED

A, gradient amplitude; FOV, field of view; MRI, magnetic resonance imaging; *R*, ramp time; RF, radio frequency; *P*, time duration of a stable gradient; SPI, single point imaging; SPRITE, single point ramped imaging with T_1 enhancement; T_E, time of echo; T_p, time of acquisition after RF excitation; T_R, time of repetition.

ACKNOWLEDGMENT

We would like to thank Prabal Ghosh of the University of Manitoba, Department of Agricultural Engineering, for measuring the water content of the seeds.

LITERATURE CITED

(1) Vertucci, C. W. The kinetics of seed imbibition. *Crop Sci. Soc. Am.* (*Seed Moisture*) **1989**, *14*, 93−115.
(2) Bewley, J. D.; Black, M. *Seeds, Physiology of Development and Germination*, 2nd ed.; Plenum: New York, 1994; Chapters 4 and 9.
(3) Davies, N. L. Patterns of hydration in barley endosperm during steeping and their relation to malting performance. In *Proceedings of the 22nd EBC Congress*; Zürich, Switzerland, VLB: Berlin, 1989; pp 221−228.
(4) Gruwel, M. L. H.; Yin, X. S.; Edney, M. J.; Schroeder, S. W.; MacGregor, A. W.; Abrams, S. Barley viability during storage: use of magnetic resonance as a potential tool to study viability loss. *J. Agric. Food Chem.* **2002**, *50*, 667−676.
(5) Hills, B. P. Food Processing-an MRI perspective. *Trends Food Sci. Technol.* **1995**, *6*, 111−117.
(6) Schmidt, S. J.; Sun, X. Z.; Lichtfield J. B. Applications of magnetic resonance imaging in food science. *Crit. Rev. Food Sci. Nutr.* **1996**, *36*, 357−385.
(7) Hills, B. P. *Magnetic Resonance Imaging in Food Science*; Wiley: New York, 1998.
(8) Bradford K. J. Manipulation of seeds water relations via osmotic priming to improve germination under stress conditions. *HortScience* **1986**, *59*, 672−676.
(9) Bray C. M. Biochemical processes during the osmopriming of seeds. In *Seed Development and Germination*; Kigil, Y., Galili, G., Eds.; Marcel Dekker: New York, 1995; Vol. 13, pp 767−789.
(10) Emid S.; Creyghton J. H. N. High-resolution NMR imaging in solids. *Physica B* **1985**, *128*, 81−83.
(11) Gravina, S.; Cory, D. G. Sensitivity and resolution of constant time imaging. *J. Magn. Reson.* **1994**, *B104*, 53−61.
(12) Mantle, M. D.; Sederman, A. J. Dynamic NMR in chemical process and reaction engineering. *Prog. NMR Spectrosc.* **2003**, *43*, 3−60.
(13) Balcom, B. J.; MacGregor, R. P.; Beyea, S. D.; Green, D. P.; Armstromg, R. L.; Bremner, T. W. Single Point Ramped Imaging with T_1 Enhancement (SPRITE) *J. Magn. Reson.* **1996**, *A123*, 131−134.
(14) Mastikhin, I. V.; Balcom, B. J.; Prado, P. J.; Kennedy, C. B. SPRITE MRI with prepared magnetizatio and centric k-space sampling. *J. Magn. Reson.* **1999**, *136*, 159−168.
(15) ASAE Moisture measurement−unground grain and seeds. In *Standards 1996*; American Society of Agricultural Engineers: St. Joseph, MI, 1996; p 387.
(16) Latta, P.; Gruwel, M. L. H.; Edie, E.; Šramek, M.; Tomanek, B. Single Point Imaging with suppressed sound pressure levels through gradient-shape adjustment. *Proc. Intl. Soc. Magn. Reson. Med.* **2004**, *11*, 2349.
(17) Ernst, R. R.; Bodenhausen, G.; Wokaun, A. *Principles of Nuclear Magnetic Resonance in One and Two Dimensions*: Oxford University Press: Oxford, 1991; pp 124−125.
(18) Woessner, D. E.; Snowden B. S., Jr. Pulsed NMR study of water in agar gels. *J. Coll. Int. Sci.* **1970**, *34*, 290−299.
(19) Brownstein, K. R.; Tarr, C. E. Importance of classical diffusion in NMR studies of water in biological cells. *Phys. Rev. A* **1979**, *19*, 2446−2453.
(20) Šramek, M.; Kaufman A. Fast ray-tracing of rectilinear volume data using distance transforms. *IEEE Trans. Vis. Comput. Graphics* **2000**, *6*, 236−252.

Received for review June 8, 2004. Accepted June 10, 2004.

JF049078F